Hamiltonian Boundary Value Method For The Nonlinear Schr ÕDinger Equation And The Korteweg-De Vries Equation

Article *in* Advances in Applied Mathematics and Mechanics · August 2017

DOI: 10.4208/aamm.2015.m1356

CITATIONS
7

READS
110

4 authors, including:

Xu Qian
National University of Defense Technology
30 PUBLICATIONS **82** CITATIONS
SEE PROFILE

Hong Zhang
National University of Defense Technology
26 PUBLICATIONS **51** CITATIONS
SEE PROFILE

Advances in Applied Mathematics and Mechanics
Adv. Appl. Math. Mech., Vol. **9**, No. 4, pp. 868-886

DOI: 10.4208/aamm.2015.m1356
August 2017

Hamiltonian Boundary Value Method for the Nonlinear Schrödinger Equation and the Korteweg-de Vries Equation

Mingzhan Song, Xu Qian, Hong Zhang and Songhe Song*

College of Science and State Key Laboratory of High Performance Computing, National University of Defense Technology, Changsha, Hunan 410073, China

Received 23 November 2015; Accepted (in revised version) 21 July 2016

Abstract. In this paper, we introduce the Hamiltonian boundary value method (HBVM) to solve nonlinear Hamiltonian PDEs. We use the idea of Fourier pseudospectral method in spatial direction, which leads to the finite-dimensional Hamiltonian system. The HBVM, which can preserve the Hamiltonian effectively, is applied in time direction. Then the nonlinear Schrödinger (NLS) equation and the Korteweg-de Vries (KdV) equation are taken as examples to show the validity of the proposed method. Numerical results confirm that the proposed method can simulate the propagation and collision of different solitons well. Meanwhile the corresponding errors in Hamiltonian and other intrinsic invariants are presented to show the good preservation property of the proposed method during long-time numerical calculation.

AMS subject classifications: 65M10, 78A48

Key words: Hamiltonian boundary value method, Hamiltonian-preserving, nonlinear Schrödinger equation, Korteweg-de Vries equation.

1 Introduction

In recent years, there exists an increasing emphasis on constructing numerical methods that can preserve structural properties of the continuous Hamiltonian systems. These methods are called geometric numerical integrators or structure-preserving numerical methods in general. Structure-preserving numerical methods originate from the numerical methods for ODEs and have a huge growth in the last decades, such as, symplectic method [1, 2], discrete gradient method [3], average vector field (AVF) [4], the HBVM [5, 6] and so on. Then people naturally pay more attention to generalising these

*Corresponding author.
Email: smz161619@163.com (M. Song), qianxu@nudt.edu.cn (X. Qian), zhanghnudt@163.com (H. Zhang), shsong@nudt.edu.cn (S. H. Song)

methods to PDEs, meanwhile, keeping geometric properties of original equations. So far, there are two main branches to preserve structures of Hamiltonian PDEs. The first is the multi-symplectic method (MSM) [7–11], which can preserve the multi-symplectic structure of the Hamiltonian system exactly. The second is Hamiltonian-preserving methods or energy-preserving methods including discrete variational derivative method [12, 13], continuous stage Runge-Kutta method [14, 15], the AVF [16–18], etc.. At present, it is widely acknowledged that Hamiltonian-preserving, as intrinsic geometric property, is of much significance during numerical simulations.

In this paper, we consider Hamiltonian system [16]

$$\frac{\partial u}{\partial t} = J\frac{\delta \mathcal{H}}{\delta u} \tag{1.1}$$

in the domain $\Omega = (x,t) \in \mathbf{R}\times\mathbf{R}$, where x and t denote space and time variables, respectively. Here, J is a constant linear skew-symmetric operator and the Hamiltonian $\mathcal{H}$ is defined as

$$\mathcal{H}[u] = \int_\Omega H(x;u,u_x,u_{xx},\cdots)dx$$

and the variational derivative [16] is given by

$$\frac{\delta \mathcal{H}}{\delta u} = \frac{\partial H}{\partial u} - \partial_x\left(\frac{\partial H}{\partial u_x}\right) + \partial_x^2\left(\frac{\partial H}{\partial u_{xx}}\right) - \cdots.$$

According to the form of (1.1), we have

$$\frac{\partial \mathcal{H}}{\partial t} = \frac{\delta \mathcal{H}}{\delta u}\frac{\partial u}{\partial t} = \frac{\delta \mathcal{H}}{\delta u}J\frac{\delta \mathcal{H}}{\delta u} = 0. \tag{1.2}$$

Obviously, the Hamiltonian is an invariant. Sometimes, Hamiltonian system can be written as

$$\frac{\partial u}{\partial t} = \mathcal{J}(u)\frac{\delta \mathcal{H}}{\delta u}, \tag{1.3}$$

where $\mathcal{J}(u)$ is a skew-symmetric operator which depends on the solution $u(x,t)$. It's easy to know, similar result can be obtain for the form of (1.3).

The HBVM was first derived for ODEs by Brugnano et al. [5] in 2009. This method has attracted much attention in recent years because of its remarkable Hamiltonian-preserving property under appropriate discretization for ODEs. In 2014, Brugnano and Sun [21] proposed a multiple invariants conserving method for Hamiltonian ODEs. Then Brugnano [20] generalised the HBVM to solve semilinear wave equation. To the best of our knowledge, this method has few applications in general nonlinear Hamiltonian PDEs and comparisons with other Hamiltonian-preserving methods. So we apply this method for the NLS and KdV equation [24–27] to show its numerical characters.

With this premise, the rest of the paper is arranged as follows. In Section 2, we review the Fourier pseudospectral method [22–24] for space-discretization and transform

the original system into a finite-dimensional Hamiltonian system. Hereafter, we introduce the HBVM in detail and apply it for the finite-dimensional system. In Section 3, the proposed method is applied for the NLS equation and KdV equation, respectively. Then numerical experiments are presented in Section 4 to show the effectiveness of the proposed method. Finally, conclusions are made in Section 5.

2 Space-discretization and time-discretization

2.1 Space-discretization by Fourier pseudospectral method

We consider the periodic boundary condition

$$u(x_L,t)=u(x_R,t)$$

and a uniform spatial grid in this paper. Dividing the interval $[x_L,x_R]$ into N equal subintervals with the space step $\Delta x=(x_R-x_L)/N$, we obtain the grid points $x_i=x_L+i\Delta x$ $(i=0,1,\cdots,N)$. Then let us introduce the vectors $\mathbf{x}=(x_0,\cdots,x_{N-1})^{\mathrm{T}}$ with $u_0(t)=u_N(t)$ and the discrete form of u is denoted by $\mathbf{u}=(u_0(t),\cdots,u_{N-1}(t))^{\mathrm{T}}$.

According to the Fourier pseudospectral method [24], we notice that the differential operator ∂_x, ∂_{xx}, ∂_{xxx} can be represented by the Fourier spectral matrices D_1, D_2, D_3 with elements

$$(D_1)_{j,l}=\begin{cases}\dfrac{1}{2}(-1)^{j+l}\mu\cot\left(\mu\dfrac{x_j-x_l}{2}\right), & j\neq l,\\ 0, & j=l,\end{cases}$$

$$(D_2)_{j,l}=\begin{cases}\dfrac{1}{2}(-1)^{j+l+1}\mu^2\csc^2\left(\mu\dfrac{x_j-x_l}{2}\right), & j\neq l,\\ -\mu^2\dfrac{(N)^2+2}{12}, & j=l,\end{cases}$$

$$(D_3)_{j,l}=\begin{cases}(-1)^{j+l}\mu^3\dfrac{\cos(\mu\frac{x_j-x_l}{2})}{\sin^3(\mu\frac{x_j-x_l}{2})}+(-1)^{j+l+1}\frac{\mu^3N^2}{8}\cot\left(\mu\dfrac{x_j-x_l}{2}\right), & j\neq l,\\ 0, & j=l,\end{cases}$$

where $j,l=1,\cdots,N$ and $\mu=2\pi/L$. It has been proved that D_1, D_3 are skew-symmetric matrices of $N\times N$ and D_2 is a symmetric matrix of $N\times N$, moreover, N must be even. These two conditions are essential for Hamiltonian-preserving. For more details, see [24] and references therein.

After space-discretization, the following finite dimensional Hamiltonian system can be obtained from (1.1):

$$\dot{\mathbf{u}}=\mathbf{J}\nabla H(\mathbf{u}), \tag{2.1}$$

where $\mathbf{J}$ is a skew-symmetric matrix. Consequently,

$$\frac{dH(\mathbf{u})}{dt}=\nabla H(\mathbf{u})^{\mathrm{T}}\dot{\mathbf{u}}=\nabla H(\mathbf{u})^{\mathrm{T}}\mathbf{J}\nabla H(\mathbf{u})\equiv 0, \tag{2.2}$$

so the Hamiltonian is still preserved after space-discretization. In the following text, mainly, we turn to solve the semi-discrete problem (2.1).

2.2 Time-discretization by Hamiltonian boundary value method

For problem (2.1), the HBVM can be used for time-discretization which allows for preservation of Hamiltonian. Let us review the approximation to the solution over the interval $[t_0,t_0+\Delta t]$. Here, we take the scaled and shifted Legendre polynomials $P_i(\xi)$ $(i=0,\cdots,n-1)$ in the interval $[0,1]$, which satisfies

$$\int_0^1 P_i(\xi)P_j(\xi)dx=\delta_{ij}=\begin{cases}1, & i=j,\\ 0, & i\neq j,\end{cases} \tag{2.3}$$

as orthonormal basis of polynomials. The basis $P_i(\xi)$ $(i=0,\cdots,n-1)$ is defined by

$$P_0=1,\quad P_i(\xi)=\sqrt{2i+1}S_i(\xi),\quad S_i(\xi)=L_i(2\xi-1), \tag{2.4}$$

$$L_i(\xi)=\frac{1}{2^i i!}\frac{d^i}{d\xi^i}(\xi^2-1)^i,\quad i=1,\cdots,n-1, \tag{2.5}$$

where $S_i(\xi)$ $(i=1,\cdots,n-1)$ is the shifted Legendre basis in the interval $[0,1]$ and $L_i(\xi)$ $(i=1,\cdots,n-1)$ is the Legendre basis in the interval $[-1,1]$. It is obvious that $degP_i(\xi)=i$ $(i=1,\cdots,n-1)$. Then the relationship of the orthonormal basis can be expressed as

$$P_0(\xi)=1,\quad P_1(\xi)=\sqrt{3}(2\xi-1),\quad P_2(\xi)=\frac{3\sqrt{5}}{2}(2\xi-1)^2-\frac{\sqrt{5}}{2},$$
$$P_{i+1}(\xi)=(2\xi-1)\frac{2i+1}{i+1}\sqrt{\frac{2i+3}{2i+1}}P_i(\xi)-\frac{i}{i+1}\sqrt{\frac{2i+3}{2i-1}}P_{i-1}(\xi),\quad i=1,\cdots,n-1.$$

In order to obtain an approximation to the true solution $\mathbf{u}(t)$ in time interval $[t_0,t_0+\Delta t]$, we apply a polynomial approximation σ, which satisfies

$$\sigma(t_0)=\mathbf{u}_0,\qquad \sigma(t_0+\Delta t)=\mathbf{u}_1.$$

The following expansions of $\dot{\sigma}(t)$, $\sigma(t)$ along the basis (2.4) for $t\in[t_0,t_0+\Delta t]$ are

$$\dot{\sigma}(t_0+c\Delta t)=\sum_{j=0}^{n-1}\gamma_j(\sigma)P_j(c),\qquad c\in[0,1], \tag{2.6a}$$

$$\sigma(t_0+c\Delta t)=\mathbf{u}_0+\Delta t\sum_{j=0}^{n-1}\gamma_j(\sigma)\int_0^c P_j(x)dx,\qquad c\in[0,1]. \tag{2.6b}$$

Then the preservation property reads

$$\begin{aligned}
&H(\boldsymbol{\sigma}(t_0+c\Delta t))-H(\boldsymbol{\sigma}(t_0))\\
=&\Delta t\int_0^1 \nabla H(\boldsymbol{\sigma}(t_0+c\Delta t))^{\mathrm{T}}\dot{\boldsymbol{\sigma}}(t_0+c\Delta t)dc\\
=&\Delta t\int_0^1 \nabla H(\boldsymbol{\sigma}(t_0+c\Delta t))^{\mathrm{T}}\sum_{j=0}^{n-1}P_j(c)\gamma_j(\boldsymbol{\sigma})dc\\
=&\Delta t\sum_{j=0}^{n-1}\Big(\int_0^1 P_j(c)\nabla H(\boldsymbol{\sigma}(t_0+c\Delta t))dc\Big)^{\mathrm{T}}\gamma_j(\boldsymbol{\sigma}).
\end{aligned}\tag{2.7}$$

It is easily checked, if we impose the following conditions

$$\gamma_j(\boldsymbol{\sigma})=\int_0^1 P_j(c)\mathbf{J}\nabla H(\boldsymbol{\sigma}(t_0+c\Delta t))dc,\quad j=0,\cdots,n-1,$$

where $\mathbf{J}$ is skew-symmetric, theoretically, we can obtain

$$\begin{aligned}
&H(\boldsymbol{\sigma}(t_0+c\Delta t))-H(\boldsymbol{\sigma}(t_0))\\
=&\Delta t\sum_{j=0}^{n-1}\Big(\int_0^1 P_j(c)\nabla H(\boldsymbol{\sigma}(t_0+c\Delta t))dc\Big)^{\mathrm{T}}\int_0^1 P_j(c)\mathbf{J}\nabla H(\boldsymbol{\sigma}(t_0+c\Delta t))dc\\
=&\Delta t\sum_{j=0}^{n-1}\Big(\int_0^1 P_j(c)\nabla H(\boldsymbol{\sigma}(t_0+c\Delta t))dc\Big)^{\mathrm{T}}\mathbf{J}\Big(\int_0^1 P_j(c)\nabla H(\boldsymbol{\sigma}(t_0+c\Delta t))dc\Big)\\
=&0.
\end{aligned}\tag{2.8}$$

By introducing γ_j in (2.6a), we can obtain,

$$\begin{aligned}
\dot{\sigma}(t_0+c_i\Delta t)=&\sum_{j=0}^{r-1}\gamma_j(\sigma)P_j(c_i)\\
=&\sum_{j=0}^{r-1}P_j(c_i)\int_0^1 P_j(c)J\nabla H(\sigma(t_0+c\Delta t))dc\\
=&\sum_{j=0}^{r-1}P_j(c_i)\Big(\sum_{l=1}^{k}\beta_l P_j(c_l)J\nabla H(\sigma(t_0+c_l\Delta t))+\Delta_j(\Delta t)\Big),
\end{aligned}\tag{2.9}$$

where β_i $(i=1,\cdots,n)$ denote the weights of the Gauss-quadrature formula corresponding to the distinct abscissae c_i $(i=1,\cdots,n)$, which are the zero points of polynomial basis $P_n(\xi)$

$$\beta_i=\int_0^1\Big(\prod_{j=1,j\neq i}^{n}\frac{x-c_j}{c_i-c_j}\Big)dx,\quad i=1,\cdots,n,$$

and $\Delta_j(\Delta t)$ denotes the error of the numerical integration formula.

In the process of numerical calculation, based on (2.6b), we ignore the tiny error of the numerical integration formula and let

$$\sigma(t_0+c_i\Delta t)=y_0+\Delta t\Big[\sum_{l=1}^{n}\beta_l\Big(\sum_{j=0}^{n-1}\int_0^{c_i}P_j(x)dxP_j(c_l)\Big)J\nabla H(\sigma(t_0+c_l\Delta t))\Big]. \tag{2.10}$$

In addition, the error of Hamiltonian (2.10) exists and can be expressed as

$$H(\mathbf{u}_1)-H(\mathbf{u}_0)=\Delta t\sum_{i=1}^{n}\beta_i\nabla H(\sigma(t_0+c_i\Delta t))^{\mathrm{T}}\dot{\sigma}(t_0+c_i\Delta t). \tag{2.11}$$

Using $\sigma(t_0+c_i\Delta t)$ obtained from (2.10), finally, the iteration formula of (2.1) has the form of

$$\mathbf{u}_1=\mathbf{u}_0+\Delta t\sum_{i=1}^{n}\beta_i\mathbf{J}\nabla H(\sigma(t_0+c_i\Delta t)). \tag{2.12}$$

For simplicity, $n\leq 3$ is considered and $n=3$ is mainly applied in the following section.

According to the numerical analysis in [20], the error of the Hamiltonian and solution error at one time step, in theory, are

$$\mathbf{u}(t_0+\Delta t)-\sigma(t_0+\Delta t)=\mathcal{O}(\Delta t^{2n+1}),\quad H(\mathbf{u}(t_0+\Delta t))-H(\sigma(t_0+\Delta t))=\mathcal{O}(\Delta t^{2n+1}). \tag{2.13}$$

Here, the original proof is omitted and more details can be seen in [5, 20] and related references.

3 HBVM for nonlinear Hamiltonian equations

In this section, the HBVM is applied to two classical examples of nonlinear Hamiltonian PDEs with periodic boundary condition: nonlinear Schrödinger (NLS) equation and Korteweg-de Vries (KdV) equation. The NLS equation is one of the most important nonlinear models in the modern science. It appears in many branches such as nonlinear quantum field theory, nonlinear optics, soliton wave, the theory of PDEs and so on. The KdV equation is a model nonlinear hyperbolic equation with smooth solutions for all times. It is widely recognised as a paradigm for the description of weakly nonlinear long waves in many branches of physics and engineering.

3.1 HBVM for the NLS equation

The NLS equation reads

$$\mathrm{i}u_t+u_{xx}+\beta|u|^2u=0, \tag{3.1}$$

where u is the complex amplitude of wave packet, $\mathrm{i}=\sqrt{-1}$ is the imaginary number, $\beta>0$ is a constant parameter. By letting $u(x,t)=p(x,t)+\mathrm{i}q(x,t)$, where $p(x,t)$ and $q(x,t)$ are real functions, we can rewrite (3.1) as a pair of real-valued equations

$$\begin{cases} p_t+q_{xx}+\beta(p^2+q^2)q=0, \\ q_t-p_{xx}-\beta(p^2+q^2)p=0. \end{cases} \tag{3.2}$$

When (3.2) is written into the form of infinite Hamiltonian system (1.1), it has

$$u=\begin{pmatrix} p \\ q \end{pmatrix}, \qquad J=\begin{pmatrix} 0 & 1 \\ -1 & 0 \end{pmatrix}, \qquad \frac{\delta\mathcal{H}}{\delta u}=\begin{pmatrix} \dfrac{\delta\mathcal{H}}{\delta p} \\ \dfrac{\delta\mathcal{H}}{\delta q} \end{pmatrix}=\begin{pmatrix} -\beta(p^2+q^2)p-p_{xx} \\ -\beta(p^2+q^2)q-q_{xx} \end{pmatrix}.$$

The Hamiltonian can be written as

$$\mathcal{H}=\int\frac{1}{2}\left[(p_x)^2+(q_x)^2-\frac{\beta}{2}(p^2+q^2)^2\right]dx. \tag{3.3}$$

By introducing the vector

$$\mathbf{u}=\begin{pmatrix} \mathbf{p} \\ \mathbf{q} \end{pmatrix}, \quad \mathbf{p}(t)=\begin{pmatrix} p_0(t) \\ \vdots \\ p_{N-1}(t) \end{pmatrix}, \quad \mathbf{q}(t)=\begin{pmatrix} q_0(t) \\ \vdots \\ q_{N-1}(t) \end{pmatrix},$$

with $p_i(t)\approx p(x_i,t)$, $q_i(t)\approx q(x_i,t)$ and $p_0(t)=p_N(t)$, $q_0(t)=q_N(t)$, we can obtain the compact form from (3.2)

$$\dot{\mathbf{u}}=\mathbf{J}\nabla H(\mathbf{u}), \quad \mathbf{J}=\frac{1}{\Delta x}\begin{pmatrix} 0 & \mathbf{I}_N \\ -\mathbf{I}_N & 0 \end{pmatrix}, \tag{3.4}$$

where $\mathbf{I}_N$ is the identity matrix of $N\times N$. The discrete form of the Hamiltonian $\mathcal{H}$ is given as

$$H(\mathbf{p},\mathbf{q})=\Delta x\left[\frac{1}{2}\left(\mathbf{p}^{\mathrm{T}}D_2\mathbf{p}+\mathbf{q}^{\mathrm{T}}D_2\mathbf{q}\right)-\sum_{j=1}^{N-1}\frac{\beta}{4}\left((p_j)^2+(q_j)^2\right)\right]. \tag{3.5}$$

More precisely, we can rewrite (3.4) in a semi-discrete form as

$$\begin{cases} \dot{\mathbf{p}}=-D_2\mathbf{q}-\beta(\mathbf{p}.^2+\mathbf{q}.^2).*\mathbf{q}, \\ \dot{\mathbf{q}}=D_2\mathbf{p}+\beta(\mathbf{p}.^2+\mathbf{q}.^2).*\mathbf{p}, \end{cases} \tag{3.6}$$

where $\mathbf{p}.^2=(p_0\times p_0,\cdots,p_{N-1}\times p_{N-1})^{\mathrm{T}}$ and $\mathbf{p}.*\mathbf{q}=(p_0\times q_0,\cdots,p_{N-1}\times q_{N-1})^{\mathrm{T}}$.

Here, we choose

$$P_0(\xi)=1, \quad P_1(\xi)=\sqrt{3}(2\xi-1), \quad P_2(\xi)=\frac{3\sqrt{5}}{2}(2\xi-1)^2-\frac{\sqrt{5}}{2},$$

as the orthonormal basis of polynomials. Then the nodes and corresponding weights of the quadrature are

$$c_1=\frac{5-\sqrt{15}}{10},\quad c_2=\frac{1}{2},\quad c_3=\frac{5+\sqrt{15}}{10},$$

and

$$\beta_1=\frac{5}{18},\quad \beta_2=\frac{4}{9},\quad \beta_3=\frac{5}{18},$$

respectively. The quadrature points are the zero points of third order scaled and shifted Legendre polynomial $P_3(\xi)=\sqrt{7}(2\xi-1)(10\xi^2-10\xi+1)$. Then (2.10) can be expressed as

$$\sigma(t_k+c_i\Delta t)=\mathbf{u}^{(k)}+\Delta t\left[\sum_{l=1}^{3}\beta_l\left(\sum_{j=0}^{2}a_{ij}P_j(c_l)\right)\mathbf{J}\nabla H(\sigma(t_k+c_l\Delta t))\right],\quad i=1,2,3, \tag{3.7}$$

where $a_{ij}=\int_0^{c_i}P_j(x)dx$ and

$$(a_{ij})_{3\times 3}=\begin{pmatrix}\frac{5-\sqrt{15}}{10} & -\frac{\sqrt{3}}{10} & \frac{\sqrt{3}}{10}\\ \frac{1}{2} & -\frac{\sqrt{3}}{4} & 0\\ \frac{5+\sqrt{15}}{10} & -\frac{\sqrt{3}}{10} & -\frac{\sqrt{3}}{10}\end{pmatrix}.$$

Analogously, we can obtain the numerical iteration formula like (2.12)

$$\mathbf{u}^{(k+1)}=\mathbf{u}^{(k)}+\Delta t\sum_{i=1}^{3}\beta_i\mathbf{J}\nabla H(\sigma(t_k+c_l\Delta t)). \tag{3.8}$$

In addition, the following global invariants [8] are also important for NLS equation (3.1)

$$\mathcal{I}_1=-\frac{1}{2}\int(p^2+q^2)dx,\quad \mathcal{I}_2=\frac{1}{2}\int(pq_x-qp_x)dx, \tag{3.9}$$

and

$$\frac{d}{dt}\mathcal{I}_1=0,\quad \frac{d}{dt}\mathcal{I}_2=0.$$

The discrete forms of $\mathcal{I}_1$ and $\mathcal{I}_2$ are

$$I_1(\mathbf{p},\mathbf{q})=-\frac{1}{2}\Delta x\sum_{j=1}^{N-1}(p_j^2+q_j^2),\quad I_2(\mathbf{p},\mathbf{q})=\frac{1}{2}\Delta x\sum_{j=1}^{N-1}\left[p_j(D_1\mathbf{q})_j+q_j(D_1\mathbf{p})_j\right]. \tag{3.10}$$

Therefore, we expect the two invariants can be preserved in the discrete form after numerical calculation. In the following section, not only the error of Hamiltonian but also the errors of I_1 and I_2 will be tested.

3.2 HBVM for the KdV equation

The KdV equation

$$u_t+\alpha uu_x+\nu u_{xxx}=0 \tag{3.11}$$

with the periodic boundary conditions can be given by bi-Hamiltonian form [19]

$$u_t=\mathcal{J}_1\frac{\delta\mathcal{H}_1}{\delta u}=\mathcal{J}_2\frac{\delta\mathcal{H}_2}{\delta u}, \tag{3.12}$$

where

$$\mathcal{J}_1=\partial_x, \qquad \mathcal{H}_1=\int\left(\frac{\nu}{2}u_x^2-\frac{\alpha}{6}u^3\right)dx, \qquad \frac{\delta\mathcal{H}_1}{\delta u}=-\nu u_{xx}-\frac{\alpha}{2}u^2,$$
$$\mathcal{J}_2=-\nu\partial_x^3-\frac{\alpha}{3}u\partial_x-\frac{\alpha}{3}\partial_x u, \qquad \mathcal{H}_2=\int\frac{1}{2}u^2dx, \qquad \frac{\delta\mathcal{H}_2}{\delta u}=u.$$

The skew-symmetric operators $\mathcal{J}_1$ and $\mathcal{J}_2$ can be discretized as skew-symmetric matrices by using the Fourier spectral matrices D_1, D_3,

$$\mathbf{J}_1=\frac{1}{\Delta x}(D_1), \quad \mathbf{J}_2=\frac{1}{\Delta x}\left(-\nu D_3-\frac{\alpha}{3}\mathbf{u}.*D_1-\frac{\alpha}{3}D_1.*\mathbf{u}^{\mathrm{T}}\right), \tag{3.13}$$

where $\mathbf{u}=(u_0,\cdots,u_{N-1})^{\mathrm{T}}$, $D_1=(d_{i,j})_{N\times N}$ and

$$\mathbf{u}.*D_1=\begin{pmatrix} d_{11}u_0 & d_{12}u_0 & \cdots & d_{1N}u_0\\ d_{21}u_1 & d_{22}u_1 & \cdots & d_{2N}u_1\\ \vdots & \vdots & \ddots & \vdots\\ d_{N1}u_{N-1} & d_{N2}u_{N-1} & \cdots & d_{NN}u_N \end{pmatrix},$$
$$D_1.*\mathbf{u}^{\mathrm{T}}=\begin{pmatrix} d_{11}u_0 & d_{12}u_1 & \cdots & d_{1N}u_{N-1}\\ d_{21}u_0 & d_{22}u_1 & \cdots & d_{2N}u_{N-1}\\ \vdots & \vdots & \ddots & \vdots\\ d_{N1}u_0 & d_{N2}u_1 & \cdots & d_{NN}u_{N-1} \end{pmatrix}.$$

Then the following finite dimensional Hamiltonian system can be obtained

$$\dot{\mathbf{u}}=\mathbf{J}_1\nabla H_1(\mathbf{u})=\mathbf{J}_2\nabla H_2(\mathbf{u}) \tag{3.14}$$

and the discrete forms of the Hamiltonian $\mathcal{H}_1$ and $\mathcal{H}_2$ are given as

$$H_1(\mathbf{u})=\Delta x\left[\frac{\nu}{2}\mathbf{u}^{\mathrm{T}}D_2\mathbf{u}-\sum_{j=1}^{N-1}\left(\frac{\alpha}{6}u_j^3\right)\right], \tag{3.15a}$$

$$H_2(\mathbf{u})=\Delta x\sum_{j=1}^{N-1}\left(\frac{1}{2}u_j^2\right). \tag{3.15b}$$

Using the same orthonormal polynomial basis of (3.8) like before, we obtain two different numerical iteration formulas corresponding to two different Hamiltonian forms

$$\mathbf{u}^{(k+1)}=\mathbf{u}^{(k)}+\Delta t\sum_{i=1}^{3}\beta_i\mathbf{J}_1\nabla H_1(\sigma(t_k+c_l\Delta t)), \tag{3.16a}$$

$$\mathbf{u}^{(k+1)}=\mathbf{u}^{(k)}+\Delta t\sum_{i=1}^{3}\beta_i\mathbf{J}_2\nabla H_2(\sigma(t_k+c_l\Delta t)). \tag{3.16b}$$

4 Numerical experiments

In this section, numerical experiments are presented for the NLS and KdV equations to illustrate the following numerical characters of the proposed method: (i) long time simulation; (ii) preservation of invariants; (iii) singularity capturing. In the following examples, the periodic boundary condition is considered and the fixed-point iteration method is applied for the three different iteration formulas (3.8), (3.16a) and (3.16b).

4.1 Numerical simulation for the NLS equation

For the NLS equation, one soliton, multiple soliton and homoclinic structure are simulated in Examples 4.1-4.3. Unless the content is stated, the standard value for the nonlinear constant in (3.1) is $\beta=2$.

Example 4.1. One soliton solution of (3.1) can be given by

$$u(x,t)=\mathrm{sech}(x-4t)\exp\left(2\mathrm{i}\left(\rho x-\frac{3}{2}t\right)\right), \tag{4.1}$$

where $\rho=1$. Here we take the value of the exact solution (4.1) at $t=0$ as our initial condition

$$u(x,0)=\mathrm{sech}(x)\cos(2x)+\mathrm{isech}(x)\sin(2x). \tag{4.2}$$

In order to show the numerical characters of the scheme (3.8), we compare it with multi-symplectic method (MSM) and average vector field (AVF) in accuracy and numerical errors of invariant quantities. The numerical iteration formula of MSM [24] is

$$\begin{cases}\dfrac{\mathbf{p}^{k+1}-\mathbf{p}^k}{\Delta t}=-D_1^2\left(\dfrac{\mathbf{q}^{k+1}+\mathbf{q}^k}{2}\right)-\beta\left(\left(\dfrac{\mathbf{p}^{k+1}+\mathbf{p}^k}{2}\right).^2+\left(\dfrac{\mathbf{q}^{k+1}+\mathbf{q}^k}{2}\right).^2\right).*\left(\dfrac{\mathbf{q}^{k+1}+\mathbf{q}^k}{2}\right),\\ \dfrac{\mathbf{q}^{k+1}-\mathbf{q}^k}{\Delta t}=D_1^2\left(\dfrac{\mathbf{p}^{k+1}+\mathbf{p}^k}{2}\right)+\beta\left(\left(\dfrac{\mathbf{p}^{k+1}+\mathbf{p}^k}{2}\right).^2+\left(\dfrac{\mathbf{q}^{k+1}+\mathbf{q}^k}{2}\right).^2\right).*\left(\dfrac{\mathbf{p}^{k+1}+\mathbf{p}^k}{2}\right),\end{cases} \tag{4.3}$$

and the numerical iteration formula of AVF [16] is

$$\begin{cases}\dfrac{\mathbf{p}^{k+1}-\mathbf{p}^k}{\Delta t}=-D_1^2\left(\dfrac{\mathbf{q}^{k+1}+\mathbf{q}^k}{2}\right)-\beta\displaystyle\int_0^1((\delta_{\mathbf{p}}^k).^2+(\delta_{\mathbf{q}}^k).^2).*\delta_{\mathbf{q}}^k d\tau,\\ \dfrac{\mathbf{q}^{k+1}-\mathbf{q}^k}{\Delta t}=D_1^2\left(\dfrac{\mathbf{p}^{k+1}+\mathbf{p}^k}{2}\right)-\beta\displaystyle\int_0^1((\delta_{\mathbf{p}}^k).^2+(\delta_{\mathbf{q}}^k).^2).*\delta_{\mathbf{p}}^k d\tau,\end{cases} \tag{4.4}$$

Table 1: Comparison of accuracy errors for the numerical solutions at $t=10$ with $\Delta t=0.001$, $\Delta x=0.25$.

method	error	p	q	$\lvert u\rvert$
HBVM	L_2	7.5320×10^{-8}	1.7225×10^{-7}	1.6165×10^{-7}
	L_∞	1.4131×10^{-8}	3.1933×10^{-8}	3.2203×10^{-8}
AVF	L_2	1.3720×10^{-4}	1.3920×10^{-4}	1.3929×10^{-4}
	L_∞	1.0757×10^{-4}	1.0264×10^{-4}	8.5964×10^{-5}
MSM	L_2	1.2608×10^{-4}	1.3141×10^{-4}	1.5010×10^{-4}
	L_∞	9.7563×10^{-5}	9.9111×10^{-5}	9.2553×10^{-5}

Table 2: Comparison of numerical errors in Hamiltonian, I_1 and I_2 at $t=10$ with $\Delta t=0.001$, $\Delta x=0.25$.

Method	error in hamiltonian	error in I_1	error in I_2
HBVM	3.5527×10^{-15}	6.6613×10^{-16}	-2.0983×10^{-13}
AVF	7.9936×10^{-15}	7.2343×10^{-12}	-3.5669×10^{-11}
MSM	1.0107×10^{-10}	3.2496×10^{-13}	-8.8107×10^{-13}

Table 3: Time accuracy test of HBVM for (3.1) with initial condition (4.1) at $T=1$ ($\Delta x=0.25$).

n	Δt	L_2 error	order	L_∞ error	order
1	0.01	1.7495×10^{-3}	-	1.2319×10^{-3}	-
	0.005	4.3713×10^{-4}	2.0008	3.0761×10^{-4}	2.0017
	0.0025	1.0914×10^{-4}	2.0019	7.6794×10^{-5}	2.0021
	0.00125	2.7154×10^{-5}	2.0069	1.9105×10^{-5}	2.0071
2	0.01	2.9804×10^{-7}	-	2.1416×10^{-7}	-
	0.005	1.8645×10^{-8}	3.9986	1.3397×10^{-8}	3.9986
	0.0025	1.1655×10^{-9}	3.9997	8.3743×10^{-10}	3.9998
	0.00125	7.2849×10^{-11}	3.9998	5.2339×10^{-11}	4.0000
3	0.01	1.3994×10^{-10}	-	8.7974×10^{-11}	-
	0.005	2.3097×10^{-12}	5.9210	1.4539×10^{-12}	5.9706
	0.0025	3.6832×10^{-14}	5.9706	2.3226×10^{-14}	5.9680
	0.00125	machine precision	-	machine precision	-

where $\delta_{\mathbf{p}}^k=(\mathbf{p}^k+\tau(\mathbf{p}^{k+1}+\mathbf{p}^k))$, $\delta_{\mathbf{q}}^k=(\mathbf{q}^k+\tau(\mathbf{q}^{k+1}+\mathbf{q}^k))$. In numerical experiment, the accuracies are tested by using the error norms L_2 and L_∞

$$L_2=\|u-\bar{u}\|_2=\left(\Delta x\sum_{j=0}^{N-1}(u_j-\bar{u}_j)^2\right)^{1/2},$$
$$L_\infty=\|u-\bar{u}\|_\infty=\max_{0\le j\le N-1}|u_j-\bar{u}_j|,$$

where Δx is the space step size, N is the number of points, u is the exact solution and $\bar{u}$ is the numerical solution. Here, we compute the numerical solutions to $t=10$ with $\Delta t=0.001$, $\Delta x=0.25$ and the CPU time of the HBVM, AVF and MSM are 40.50, 22.01 and 34.68, respectively. The comparison of accuracy errors are shown in Table 1. The

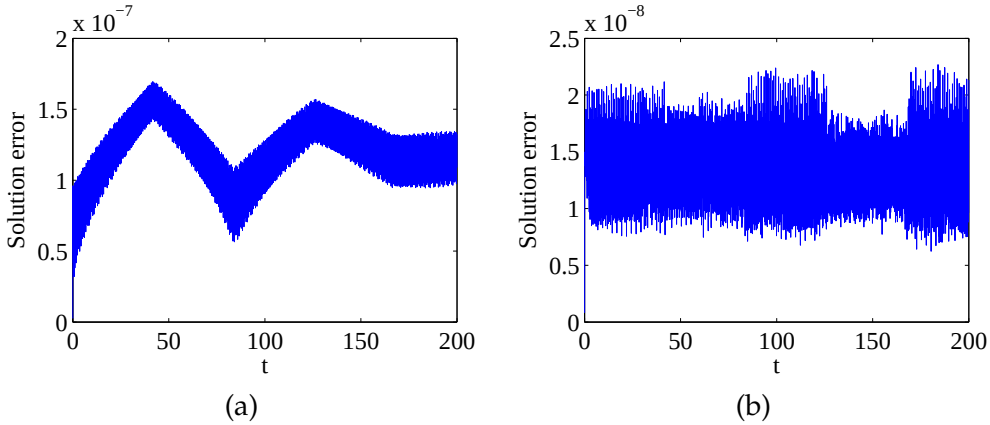

Figure 1: L_2 error (a) and L_∞ error (b) of numerical solution.

HBVM scheme has much higher accuracy than the AVF scheme and MSM scheme without costing much more CPU time. Table 2 shows the errors in Hamiltonian, I_1 and I_2 of the three different schemes. At the same time, we also find the HBVM scheme more effective than the other two schemes in preserving not only the Hamiltonian but also other two invariant quantities. To reflect the character of long time simulation and invariants preserving of the proposed method more fully, we let $t\in[0,200]$ with the same time and space step. The numerical solution errors are shown in Fig. 1, meanwhile, the errors of the Hamiltonian, I_1 and I_2 are only -7.9936×10^{-15}, 9.3259×10^{-15} and -1.2701×10^{-13} at $t=200$. The time accuracy of the proposed method with $n=1,2,3$ is tested. The L_2 and L_∞ errors, as well as the numerical order of accuracy, are contained in Table 3. The numerical results approximatively consistent with theoretical $2n$ order time accuracy. Simultaneously, when $\Delta t=0.01$, the error of Hamiltonian can reach the magnitude of 10^{-4}, 10^{-8} and 10^{-12} corresponding to $n=1,2,3$.

Example 4.2. Consider the multiple soliton elastic collision of (3.1) with the symmetric initial condition

$$u(x,0)=\sum_{i=1}^{n}\operatorname{sech}(x-x_i)\exp\left(\frac{1}{2}i(\rho_i(x-x_i))\right). \tag{4.5}$$

First, we set $\Delta t=0.001$ and $N=200$. The computational domain is $[-25,25]$ and the time interval is $[0,50]$. When we let $n=2$, $\rho_1=4$, $\rho_2=-4$, $x_1=-10$, $x_2=10$, the nonlinear wave propagation is double soliton head-on collision. Fig. 2 displays the numerical solutions till time $T=50$, where the left upper side is time evolution of the collision, the right upper side is the corresponding contour picture in phase space and the bottom is the waveform at $t=0.5$, $t=2.0$, $t=2.5$, $t=4.0$. As we can see, the motions of the two solitons are preserved very well. Fig. 3 gives the numerical errors in Hamiltonian, I_1 and I_2. Compared with the symplectic wavelet collocation method in [8], the proposed method is more effective to preserve the three invariant quantities. Similarly, when we let $n=2$,

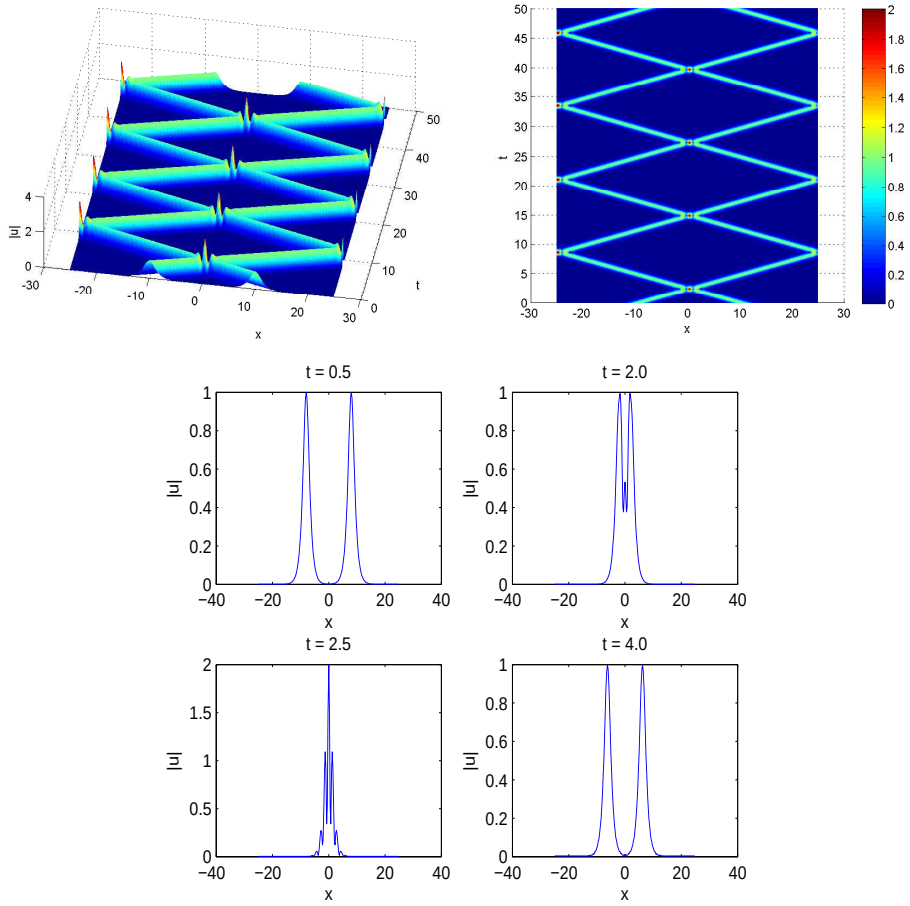

Figure 2: The double soliton head-on elastic collision of (3.1) with initial condition (4.5).

$\rho_1=5$, $\rho_2=0.5$, $x_1=-15$, $x_2=0$, the nonlinear wave propagation is catching-up collision shown in the left side of Fig. 4. The magnitude of numerical errors in Hamiltonian, I_1 and I_2 is 10^{-14}, 10^{-14}, 10^{-4} respectively. Then, we refine the grid to $N=500$ and keep the time step. The numerical solution of the treble soliton elastic collision with $n=3$, $\rho_1=5$, $\rho_2=0$, $\rho_3=-5$, $x_1=-15$, $x_2=0$, $x_3=15$ is plotted in the right side of Fig. 4. The magnitude of numerical errors in Hamiltonian, I_1 and I_2 is 10^{-13}, 10^{-15}, 10^{-11} respectively.

Example 4.3. We discuss the bound state solution of (3.1) with initial condition

$$u(x,0)=\operatorname{sech}(x). \tag{4.6}$$

It will produce a bound state of K solitons when $\beta=2K^2$. As for $K\geq 3$, the solutions are difficult to resolve because of large spatial and temporal gradients in the solution. For the case $\beta=2\times 5^2$, this problem will produce a bound state of 5 solitons. The problem is solved in $[-15,15]\times[0,10]$ with $\Delta t=0.0001$ and $N=960$. It has a periodic solution

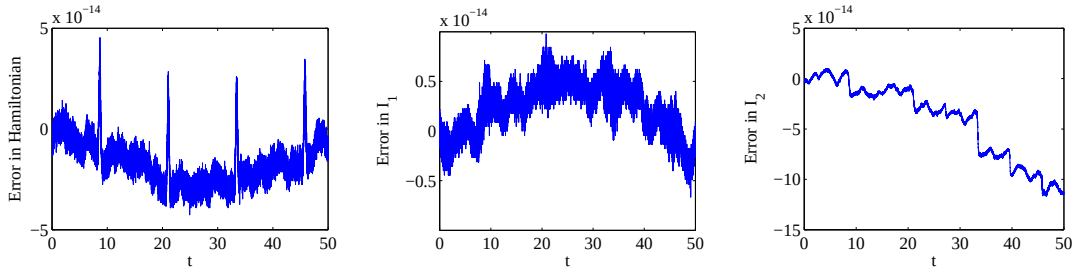

Figure 3: The variation of errors in Hamiltonian, I_1 and I_2.

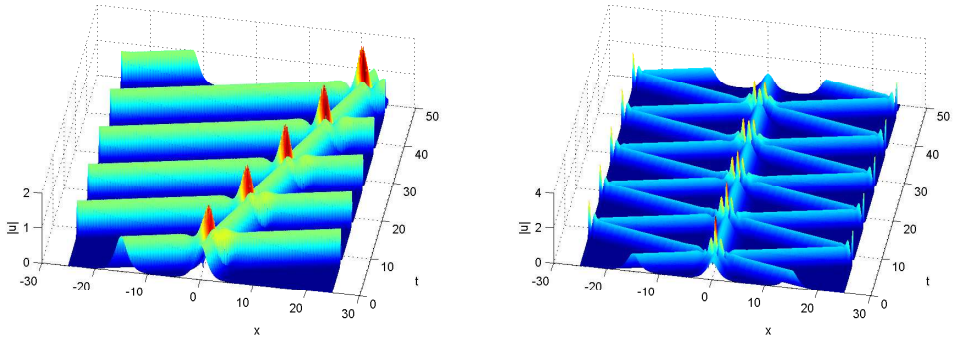

Figure 4: The double soliton catching-up elastic collision and the treble soliton elastic collision of (3.1) with initial condition (4.5).

with period of $L \approx 0.7854$. In Fig. 5, time evolution of the bound state solution and corresponding contour pictures is shown over $t \in [0,10]$, the waveform is at $t=0$, $t=0.19$, $t=0.395$, $t=0.6$ in the first period. Although the soliton is sharp, the proposed method simulates the evolution of the five-soliton bound state solution very well, which reflects the high capacity of singularity capturing of the proposed method. The numerical errors in the three invariant quantities can be found in Fig. 6. Again, the errors in I_1 and I_2 are negligible and the error in total Hamiltonian is bounded.

4.2 Numerical simulation for the KdV equation

For the KdV equation, we take single soliton and triangular periodic solution as example, which can reflect the effectiveness of proposed method.

Example 4.4. Consider the single soliton propagation with $\alpha=1$, $\nu=6$ under the initial condition

$$u(x,0)=\operatorname{sech}^2\left(\frac{x}{\sqrt{2}}\right). \tag{4.7}$$

In this example, numerical simulation is made with $\Delta x=0.2$ and $\Delta t=0.001$ in $[-20,20]\times[0,200]$. Fig. 7 shows the waveform at $t=0$ and $t=200$ and the numerical

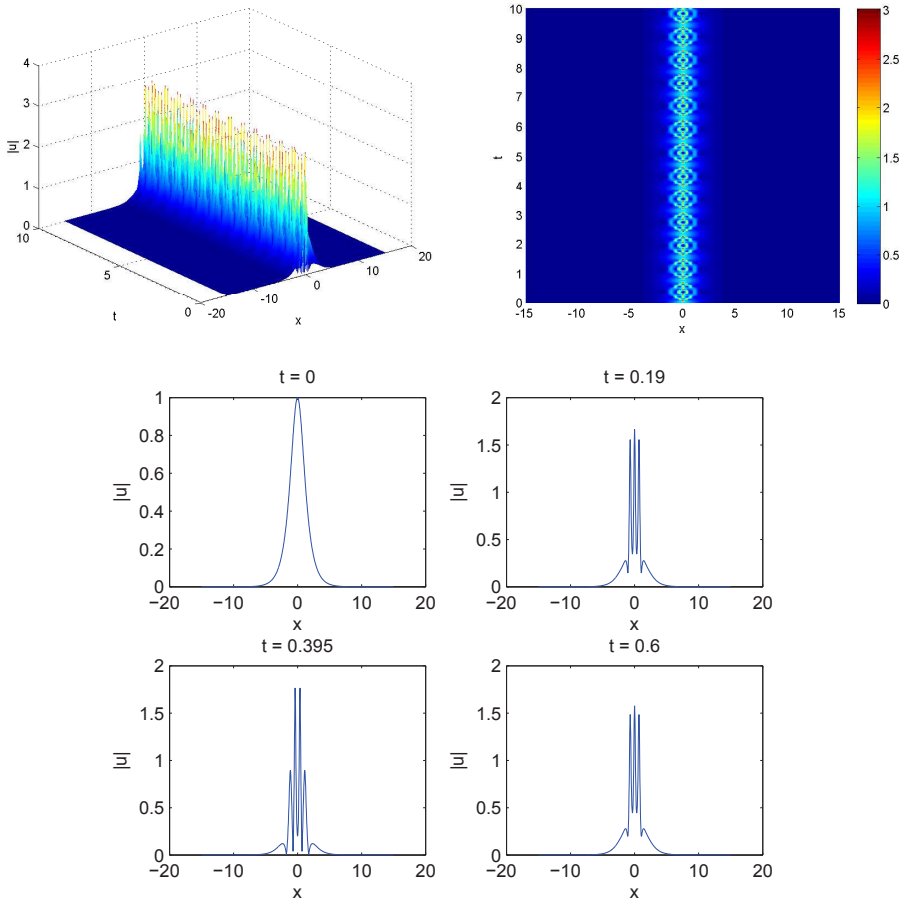

Figure 5: The nonlinear wave propagation of (3.1) with initial condition (4.6) ($\Delta t = 0.0001$, $N = 960$).

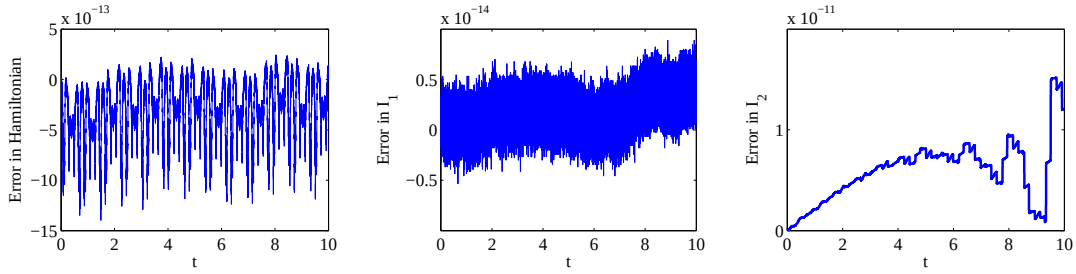

Figure 6: The variation of errors in Hamiltonian, I_1 and I_2 ($\Delta t = 0.0001$, $N = 960$).

result is still stable after long time numerical simulation. The errors of Hamiltonian H_1 and H_2 during [0,200] are shown in Fig. 8, which indicate the character of Hamiltonian preserving of the proposed method.

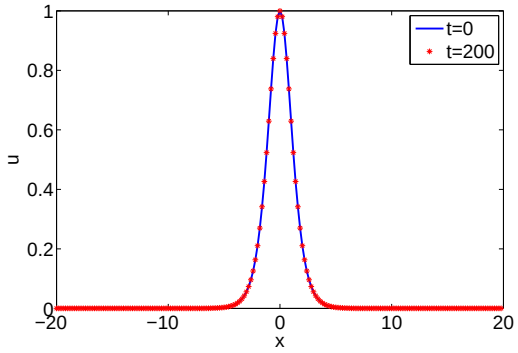

Figure 7: Numerical solutions of (3.11) with initial condition (4.7) at $t=200$.

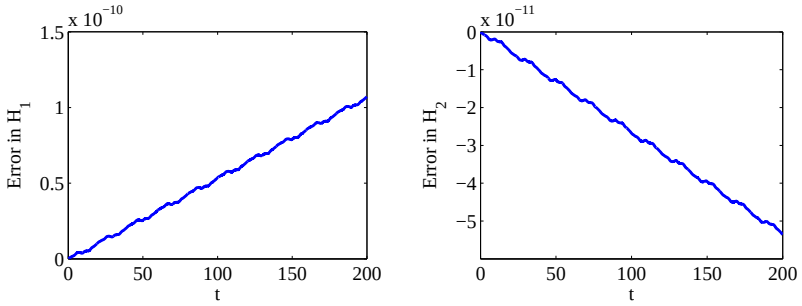

Figure 8: The variation of errors in H_1 and H_2.

Example 4.5. We set $\alpha=0.022^2$, $\nu=1$ and take the triangular periodic initial condition

$$u(x,0)=\cos(\pi x). \tag{4.8}$$

Here, we use the same step sizes $\Delta x=0.01$ and $\Delta t=0.0001$ as in [25] in the interval $x\in[0,2]$. The computations are done with respect to the two Hamiltonian pairs of KdV equation (3.11) till $T=20$. Fig. 9 shows solutions of the KdV equation using the scheme (3.16a), which shows a similar solutions as with those obtained by the MSM in [25] and AVF methods in [19] for the same time snapshots. Similar solutions are obtained for the second Hamiltonian formulation (3.16b). The error in the Hamiltonian H_1 and H_2 are shown in Fig. 10. It is certain that the proposed method also have satisfactory results with solitary wave.

5 Conclusions

In this paper, we have applied a new scheme for the nonlinear Hamiltonian PDEs with periodic boundary condition. We got this scheme based on the Fourier pseudospectral method in space and the Hamiltonian boundary value method in time. The numerical

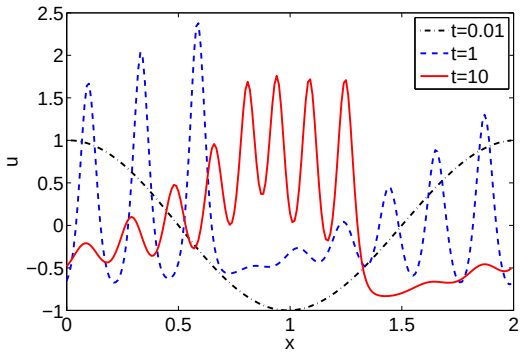

Figure 9: Numerical solutions of (3.11) with initial condition (4.8) at various times $t=0.01$, $t=1$ and $t=10$.

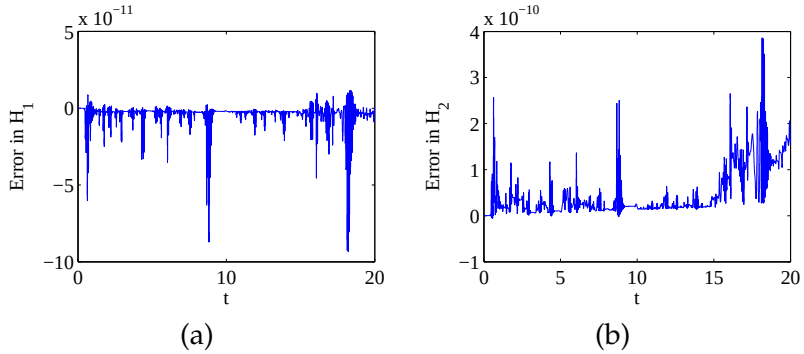

Figure 10: The variation of error in H_1 and H_2.

results of the NLS equation and the KdV equation show that the proposed method is able to preserve not only the shapes and velocities of solutions of the nonlinear Hamiltonian PDEs even after collision but also the Hamiltonian and other invariant quantities. By comparison, we can see the proposed method is more effective than the traditional multi-symplectic scheme and AVF scheme in long-time numerical simulation. Furthermore, this method is also better than symplectic wavelet collocation method in preserving Hamiltonian, I_1 and I_2, which is of great importance in simulations.

Acknowledgments

This work is supported by the Natural Science Foundation of China (Grant Nos. 11571366, 11501570) and the Open Foundation of State Key Laboratory of High Performance Computing of China.

References

[1] R. McLachlan, *Symplectic integration of Hamiltonian wave equations,* Numerische Mathematik, 66(1) (1993), pp. 465–492.

[2] K. Feng and M. Z. Qin, *Symplectic difference schemes for Hamiltonian systems,* in Symplectic Geometric Algorithms for Hamiltonian Systems, Springer Berlin Heidelberg, (2010), pp. 187–211.

[3] M. Dahlby, B. Owren and T. Yaguchi, *Preserving multiple first integrals by discrete gradients,* J. Phys. A Math. Theor., 44(30) (2011), 305205.

[4] G. R. W. Quispel and D. I. McLaren, *A new class of energy-preserving numerical integration methods,* J. Phys. A Math. Theor., 41(4) (2008), 045206.

[5] L. Brugnano, F. Iavernaro and D. Trigiante, *Hamiltonian boundary value methods (energy preserving discrete line integral methods),* J. Numer. Anal. Industrial Appl. Math., 5(1-2) (2010), pp. 17–37.

[6] L. Brugnano and F. Iavernaro, *Line integral methods which preserve all invariants of conservative problems,* J. Comput. Appl. Math., 236(16) (2012), pp. 3905–3919.

[7] T. J. Bridges and S. Reich, *Multi-symplectic integrators: numerical schemes for Hamiltonian PDEs that conserve symplecticity*, Phys. Lett. A, 284 (2001), pp. 184–193.

[8] H. J. Zhu, L. Y. Tang, S. H. Song, Y. F. Tang and D. S. Wang, *Symplectic wavelet collocation method for Hamiltonian wave equations,* J. Comput. Phys., 229 (2010), pp. 2550–2572.

[9] X. Qian, S. H. Song and E. Gao, *Explicit multi-symplectic method for the Zakharov-Kuznetsov equation,* Chinese Phys. B, 21(7) (2012), pp. 43–48.

[10] H. C. Li, J. Q. Sun and M. Qin, *Multi-symplectic method for the Zakharov-Kuznetsov equation,* Adv. Appl. Math. Mech., 7(1) (2015), pp. 58–73.

[11] X. Qian, S. H. Song and Y. M. Chen, *A semi-explicit multi-symplectic splitting scheme for a 3-coupled nonlinear Schrödinger equation,* Comput. Phys. Commun., 185(4) (2014), pp. 1255–1264.

[12] Y. Takaharu, T. Matsuo and M. Sugihara, *The discrete variational derivative method based on discrete differential forms,* J. Comput. Phys., 231(10) (2012), pp. 3963–3986.

[13] Y. Miyatake and T. Matsuo, *Conservative finite difference schemes for the Degasperis-Procesi equation,* J. Comput. Appl. Math., 236(15) (2012), pp. 3728–3740.

[14] E. Hairer, *Energy-preserving variant of collocation methods,* J. Numer. Anal. Industrial Appl. Math., 5 (2010), pp. 73–84.

[15] Y. Miyatake, *An energy-preserving exponentially-fitted continuous stage Runge-Kutta method for Hamiltonian systems*, BIT Numer. Math., 54(3) (2014), pp. 777–799.

[16] E. Celledoni, V. Grimm, R. I. McLachlan, D. I. McLaren, D. O'Neale, B. Owren and G. R. W. Quispel, *Preserving energy resp. dissipation in numerical PDEs using the "Average Vector Field" method,* J. Comput. Phys., 230(20) (2012), pp. 6770–6789.

[17] H. Zhang and S. H. Song, *Average vector field methods for the coupled Schrödinger KdV equations,* Chinese Phys. B, 23(7) (2014), pp. 242–250.

[18] J. X. Cai, Y. S. Wang and Y. Z. Gong, *Numerical analysis of AVF methods for three-dimensional time-domain Maxwell's equations,* J. Sci. Comput., (2015), pp. 1–36.

[19] B. Karasozen and G. Simsek, *Energy preserving integration of bi-Hamiltonian partial differential equations,* Appl. Math. Lett., 26(12) (2013), pp. 1125–1133.

[20] L. Brugnano, G. F. Caccia and F. Iavernaro, *Energy conservation issues in the numerical solution of the semilinear wave equation*, Appl. Math. Comput., 270(C) (2015), pp. 842–870.

[21] L. Brugnano and Y. J. Sun, *Multiple invariants conserving Runge-Kutta type methods for*

Hamiltonian problems, Numer. Algorithms, 65(3) (2014), pp. 611–632.
[22] Y. M. CHEN, S. H. SONG AND H. J. ZHU, *Explicit multi-symplectic splitting methods for the nonlinear Dirac equation,* Adv. Appl. Math. Mech., 6(4) (2014), pp. 494–514.
[23] Y. M. CHEN, S. H. SONG AND H. J. ZHU, *Multi-symplectic methods for the Ito-type coupled KdV equation,* Appl. Math. Comput., 218(9) (2012), pp. 5552–5561.
[24] J. B. CHEN AND M. Z. QIN, *Multi-symplectic fourier pseudospectral method for the nonlinear Schrödinger equation,* Electronic Transactions on Numerical Analysis, 12 (2001), pp. 193–204.
[25] U. M. ASCHER AND R. I. MCLACHLAN, *On symplectic and multisymplectic schemes for the KdV equation,* J. Sci. Comput., 25(1) (2005), pp. 83–104.
[26] L. L. WEI, Y. N. HE AND X. D. ZHANG, *Analysis of an implicit fully discrete local discontinuous Galerkin method for the time-fractional Kdv equation,* Adv. Appl. Math. Mech., 7(4) (2015), pp. 510–527.
[27] E. KIERI, G. KREISS AND O. RUNBORG, *Coupling of Gaussian beam and finite difference solvers for semiclassical Schrödinger equations,* Adv. Appl. Math. Mech., 7(6) (2015), pp. 687–714.